Ogawa *et al. Earth, Planets and Space* (2022) 74:153
https://doi.org/10.1186/s40623-022-01713-3

Earth, Planets and Space

FULL PAPER

Particle size distributions inside and around the artificial crater produced by the Hayabusa2 impact experiment on Ryugu

K. Ogawa[1,2], N. Sakatani[3], T. Kadono[4*], M. Arakawa[2], R. Honda[5], K. Wada[6], K. Shirai[2], Y. Shimaki[3], K. Ishibashi[6], Y. Yokota[3], T. Saiki[3], H. Imamura[3], Y. Tsuda[3], S. Nakazawa[3], Y. Takagi[7], M. Hayakawa[3], H. Yano[3,8], C. Okamoto[2], Y. Iijima[3], T. Morota[9], S. Kameda[10], E. Tatsumi[9,11], Y. Cho[9], K. Yoshioka[16], H. Sawada[3], M. Matsuoka[12], M. Yamada[6], T. Kouyama[13], H. Suzuki[14], C. Honda[15] and S. Sugita[6,9]

Abstract

Japanese Hayabusa2 spacecraft has successfully carried out an impact experiment using a small carry-on impactor (SCI) on an asteroid (162173) Ryugu. We examine the size distribution of particles inside and outside an artificial impact crater (the SCI crater) based on the images taken by the optical navigation camera onboard the Hayabusa2 spacecraft. The circumferential variation in particle size distribution inside the SCI crater is recognized and we interpret that major circumferential variation is caused by the large boulders inside the SCI crater that existed prior to the impact. The size distribution inside the SCI crater also shows that the subsurface layer beneath the SCI impact site had a large number of particles with a characteristic size of ~9 cm, which is consistent with the previous evaluations. On the other hand, the size distribution outside the SCI crater exhibits the radial variation, implying that the deposition of ejecta from the SCI crater is involved. The slope of the size distribution outside the crater at small sizes differs from the slope of the size distribution on the surface of Ryugu by approximately 1 or slightly less. This is consistent with the claim that some particles are buried in fine particles of the subsurface origin included in ejecta from the SCI crater. Thus, the particle size distributions inside and outside the SCI crater reveal that the subsurface layer beneath the SCI impact site is rich in fine particles with ~9 cm in size while the particles on the surface have a size distribution of a power-law form with shallower slopes at small sizes due to the deposition of fine ejecta from the subsurface layer. Finally, we discuss a process responsible for this difference in particle size distribution between the surface and the subsurface layers. The occurrence of segregation in the gravitational flow of particles on the surface of Ryugu is plausible.

Keywords: Asteroid Ryugu, SCI crater, Particle size distribution, Ejecta deposition

*Correspondence: kadono@med.uoeh-u.ac.jp

[4] Department of Basic Sciences, University of Occupational and Environmental Health, Kitakyusyu, Japan
Full list of author information is available at the end of the article

Graphical Abstract

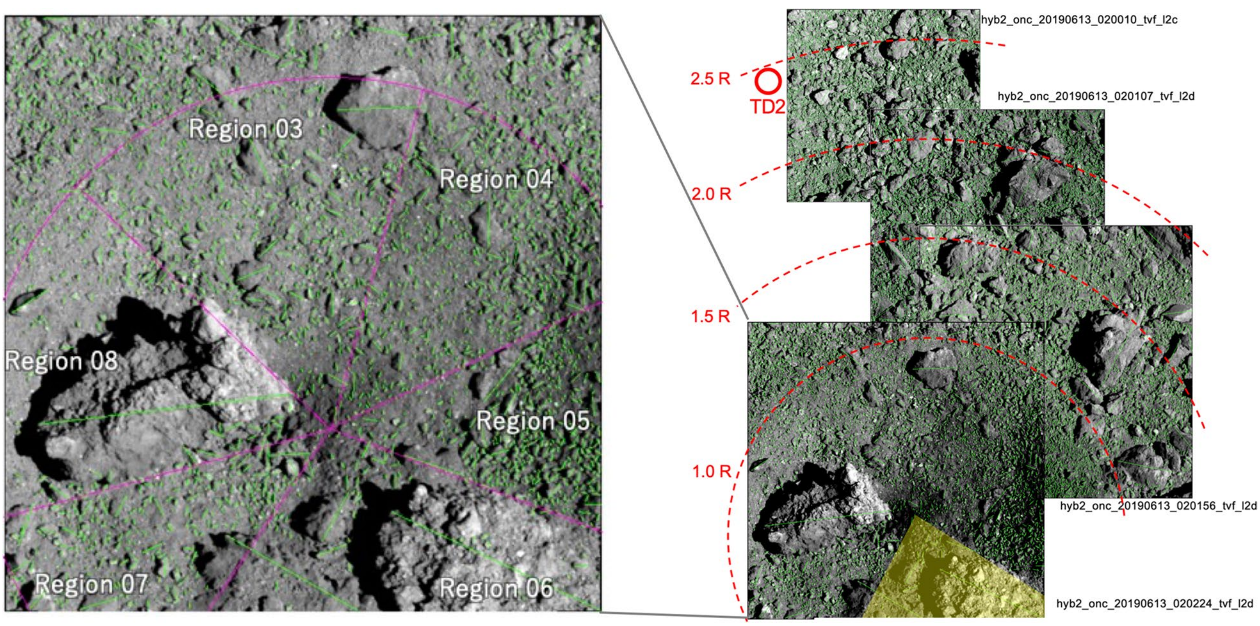

Introduction

In April 2019, the Hayabusa2 spacecraft succeeded in an impact experiment using a small carry-on impactor (SCI) on the asteroid Ryugu (Arakawa et al. 2020) and an artificial crater, so called the SCI crater, was formed at latitude 7.9°N and longitude 301.3°E (local height and slope around the SCI impact site are shown in Arakawa et al. (2020) and Additional file 1: Fig. S1, respectively). Arakawa et al. (2020) investigated the size–frequency distribution of particles within the crater. They showed that the particle size distribution inside the crater differs from that on the typical surface of Ryugu and that the wall of the SCI crater, which corresponds to the subsurface layer of Ryugu, is primarily composed of regolith particles with sizes smaller than 0.2 m. This is confirmed by in situ observations of the ejecta curtain caused by the SCI impact (Kadono et al. 2020b; Wada et al. 2021): The size of particles in the ejecta curtain is estimated to be several centimeters (Wada et al. 2021). Thus, it is likely that Ryugu has a layered structure and that there is a large number of small particles, whose size has been determined only in orders of magnitude, in the subsurface layer.

The surface of Ryugu is covered with many large boulders (Sugita et al. 2019). The size distribution of boulders has a power-law form, but the slope of the cumulative size distribution gradually changes with size from -2.65 ± 0.05 for large boulders (> -5 m) to -1.65 ± 0.05 for small particles (0.02–3.3 m) (Sugita et al. 2019; Michikami et al. 2019). Sugita et al. (2019) and Michikami et al. (2019) claim that, since several close-up images indicate that some of particles are buried, the change in the slope is caused by finer ejecta particles from nearby craters burying such smaller particles. In fact, ejecta blanket is deposited around the SCI crater: Arakawa et al. (2020) analyzed the patterns of the ejecta curtain evolving through time together with the reflectance difference map of the surface around the SCI crater and found that regions showing a larger decrease in reflectance factor are consistent with the non-uniform pattern of the ejecta curtain, implying that the region with a lower reflectance has to be covered with thicker ejecta deposits. The change in size distribution of the surface layer particles due to the deposition of the subsurface layer particles also suggests that Ryugu has a layered structure with the different size distribution of the surface layer and the subsurface layer.

Kadono et al. (2020b) proposed three hypotheses for the geological process that formed the subsurface structure beneath the SCI impact point: (i) vertical size segregation in the mass flow on the surface of Ryugu; (ii) scraping weak base rocks by mass flow; and (iii) thermal fatigue of base rocks by diurnal temperature and subsequent mass flow. In hypotheses (ii) and (iii), some particles with a characteristic size are newly added to the mass flow, so the size distribution of particles in the subsurface layer is larger in some size ranges than the original size distribution in the mass flow. On the other hand, in hypothesis (i), the size distribution in the subsurface layer is always lower than the original distribution, because the particles in the subsurface layer are part of the particles in the mass flow. The detailed analysis of the size distribution would allow us to discuss which model is more plausible.

In this paper, we examine the size distributions inside and outside the SCI crater in detail, and, using these results, we investigate the particle size distributions on the surface layer and in the subsurface layer at the SCI impact site. First, we report the results of a detailed analysis of the size distribution of particles inside and outside the SCI crater. Arakawa et al. (2020) has only provided preliminary results on the size distribution. We show the radial and azimuthal variation of the particle size distribution. Next, we evaluate the difference in size distribution between the surface layer and the subsurface layer based on the size distributions inside and outside the SCI crater. We identify the characteristic size of the materials in the subsurface layer, which has been determined only in orders of magnitude. Then, we verify if the change in the slope of the size distribution outside the SCI crater at small sizes is caused by the deposition of ejecta from the subsurface layer with a different size distribution. Finally, we discuss the physical process at the Ryugu surface that produces the difference in size distribution between the surface and subsurface layers. Ryugu is a top-shaped asteroid (Watanabe et al. 2019) and various mechanisms responsible for the formation of top-shaped asteroids have been proposed such as fast rotation (e.g., Walsh et al. 2008; Harris et al. 2009), internal structural deformation (e.g., Hirabayashi and Scheeres 2019), and reaccumulation (e.g., Michel et al. 2020). The process should be consistent with such mechanism. In this paper, we discuss the process, supposing that Ryugu was fast rotating.

In the next section, we describe the images we analyzed. Then, we show the particle size distributions inside and outside the SCI crater and the difference between these distributions in the Result section. In the Discussion section, first, we evaluate the characteristic size of particles in the subsurface layer, and second, the effect of ejecta deposition on the particle size distributions is shown. Then, the process which caused the differences in particle size distributions of surface and subsurface is discussed. Finally, we summarize this paper in the Summary section.

Image analyses

The images used for particle size measurement were taken by the optical navigation camera (ONC-T; Kameda et al. 2017) acquired during an operation of close-up observation (PPTD-TM1B) on June 13, 2019, which was performed in a touchdown rehearsal and target marker separation (Kikuchi et al. 2022). The ONC-T on the spacecraft imaged the area around the SCI crater at an altitude of about 100 m in this operation with a spatial resolution of about 1 cm/pix. We analyzed four images hyb2_onc_20190613_020010_tvf_l2c.fit, hyb2_onc_20190613_020107_tvf_l2c.fit, hyb2_onc_20190613_020156_tvf_l2c.fit, and hyb2_onc_20190613_020224_tvf_l2c.fit. The altitudes of the spacecraft and the ONC-T spatial resolutions are summarized in Table 1. These images have overlapped regions so that we produce a composite image that covers the SCI crater and its northern area (Fig. 1). The rim of the SCI crater is indicated by a red broken semi-circle with the label of 1.0R, where R denotes the radius of the SCI crater. The longest length of the particles in each image was individually and manually measured on the SAOImageDS9 image visualization software. The measured particles are marked with a green line, indicating their longest length. It should be noted that the yellow-hatched area on the south side of the crater is a "forbidden zone" in which the crater formation process did not occur because of the large boulder (Arakawa et al. 2020). Hence, we did not include the particles in this area.

First, we investigated the radial variation of the particle size distributions (Fig. 2a). Four size distributions of particles were examined at the distance between 1.0R and 1.5R, 1.5R and 2.0R, 2.0R and 2.5R, and 2.5R and 3.0R from the SCI crater center. Then, we examined the size distribution of particles inside the crater in 6 separate regions, which are defined as a fan shaped region bounded by 6 purple lines drawn from the crater center radially as shown in Fig. 3a, and each region is named R03–R08 clockwise. The circumferential variation of the particle size distribution was obtained (Fig. 3b).

Results

Radial variation of particle size distribution outside the SCI crater

Figure 2a shows a radial variation of particle size distribution outside the SCI crater. To make the variation

Table 1 Images used in the particle size counting

Image ID	Spacecraft altitude [m]	Spatial resolution [mm/pix]
hyb2_onc_20190613_020010_tvf_l2c	80	8.5
hyb2_onc_20190613_020107_tvf_l2c	96	10.3
hyb2_onc_20190613_020156_tvf_l2c	108	11.6
hyb2_onc_20190613_020224_tvf_l2c	117	12.6

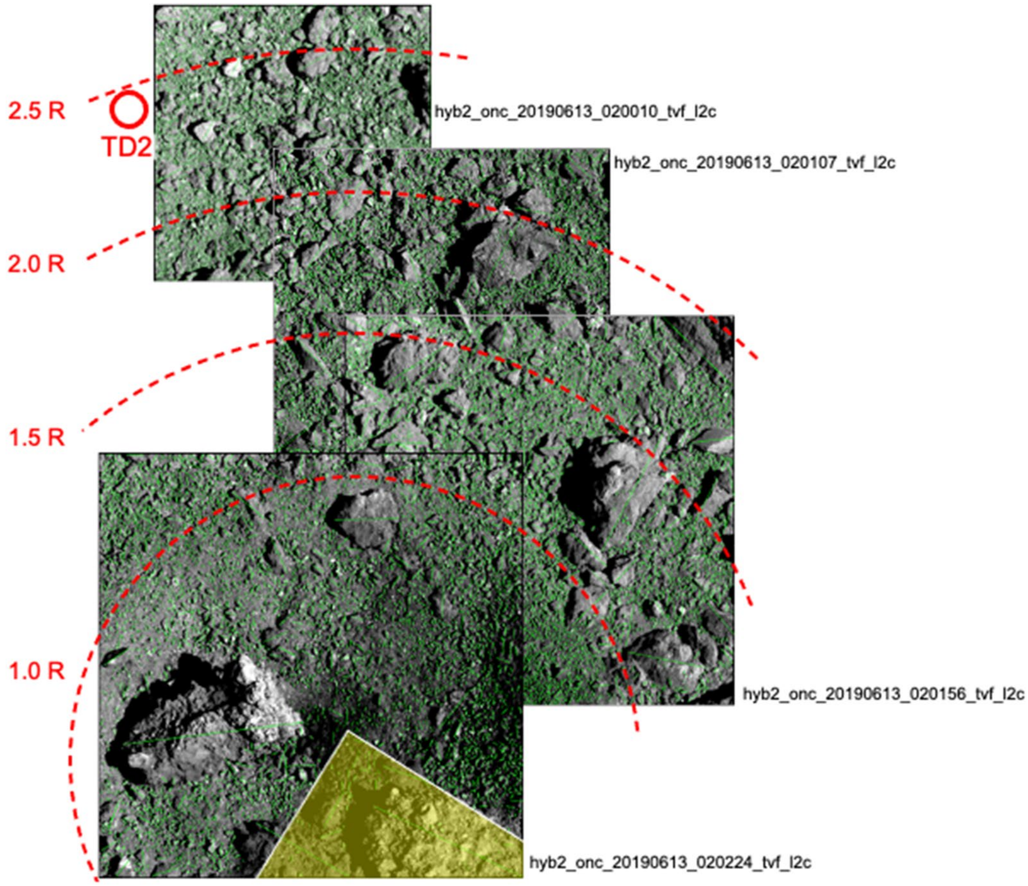

Fig. 1 Analyzed images in this study: hyb2_onc_20190613_020010_tvf_l2c.fit, hyb2_onc_20190613_020107_tvf_l2c.fit, hyb2_onc_20190613_020156_tvf_l2c.fit, and hyb2_onc_20190613_020224_tvf_l2c.fit, obtained at PPTD-TM1B. The rim of the SCI crater is indicated as a broken semi-circle with a mark of 1.0R. Semi-circles with a label of 1.5R, 2.0R, and 2.5R represent concentric circles centered on the impact point. The yellow-hatched area in the south of the impact point is a forbidden zone at which no cratering process occurred due to the large boulder near the impact point (Arakawa et al. 2020). We did not include the particles in this yellow-hatched area. A red circle labeled "TD2" indicates the location at which the second touchdown and the sampling were conducted

easier to see, we show relative cumulative frequency between 0.1 and 1.0 m obtained by dividing each cumulative distribution by the cumulative distribution of particles within the innermost annulus of 1.0R–1.5R every 0.1 m in Fig. 2b. The relative frequency depends on the distance from the crater: a higher abundance of particles is recognized far from the crater at small sizes at least below ‒ 0.5 m. This implies that the deposition of ejecta from the crater is involved. It is noted that the relative frequency still changes even in 2.0R–3.0R. Since the second sampling point located in 2.0R–2.5R ("TD2" in Fig. 1), it is suggested that the ejecta from the SCI crater exists around the TD2 point. Hence, the returned samples from Ryugu to Earth should include the materials from the SCI crater.

Circumferential variation of particle size distribution inside the SCI crater

Figure 3b shows the size frequency distributions of particles in each azimuthal segment inside the SCI crater. It is noticeable that the distribution is somewhat dependent on the locality. The distributions of Regions 06 and 08 are rather lower than those of others and show one order of magnitude lower than those in other regions because these regions include large boulders with a size larger than 5 m, such as Okamoto boulder and Iijma boulder; they dominate most of these regions, reducing the particle numbers. In order to exclude the effect of Iijima boulder on the particle size frequency distribution of Region 08, the distribution was calculated at the area without Iijima boulder (R08s of Fig. 3c). Thus, we noticed

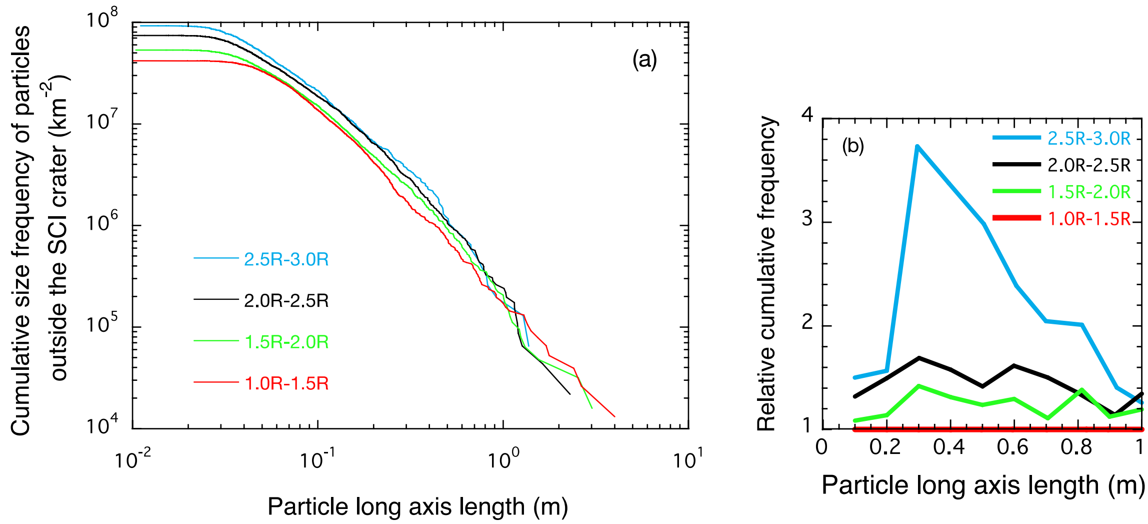

Fig. 2 **a** Radial variation of cumulative size–frequency distributions of particles located within the annulus of 1.0R–1.5R, 1.5R–2.0R, 2.0R–2.5R, and 2.5R–3.0R. **b** Each cumulative frequency in **a** is divided by the cumulative frequency of particles within the innermost annulus of 1.0R–1.5R every 0.1 m

that the particle number density outside of Iijima boulder in Region 08 is almost consistent with Region 03 at the particle size larger than 20 cm but it is still smaller than that of its neighboring region (Region 03) at the particle size smaller than 20 cm. In the east area of Region 05, it is very clear by eye that the number density of particles with the size of a few cm is higher than that in the crater center of Region 05. Furthermore, we can recognize a lot of particles that are not buried in the crater wall in this east area (Fig. 3c): they look loose and not completely attached to the wall, so these particles might have rolled down from the higher area of the east slope due to the collapse of the deposited rim and were left on the wall. While the crater walls of Regions 03, 04, and 07 look so smooth because most of the particles are buried in the walls (Fig. 3c).

The difference between the size distributions inside and outside the SCI crater

We consider the sum of four distributions shown in Fig. 2a and the sum of the 6 distributions of particles shown in Fig. 3b as typical distributions outside and inside the SCI crater, respectively (Fig. 4). They intersect at ~ 2–3 m, but the size distribution inside the crater is always lower than the distribution outside the crater at sizes < 1 m, though it asymptotically approaches at sizes < ~ 0.1 m. Arakawa et al. (2020) stated a higher abundance of particles for the distribution outside the SCI crater, especially, at several decimeters. The results obtained by the detailed analysis shown in Fig. 4 support this statement. Using the least squares method, the slope of the distribution of particles outside the crater with sizes larger than 0.5 m is obtained to be − 2.45 while the slope between 0.1 and 0.5 m is obtained to be shallower − 1.75. The fact that the slope becomes shallower at smaller sizes is consistent with the results obtained by Michikami et al. (2019) for small particles − 1.65 (0.02–3.3 m in size) and − 2.01 (0.1–4.1 m in size).

Discussion

Size distribution of particles in the subsurface layer

Ryugu has a layered structure on the surface (e.g., Kadono et al. 2020b). The outermost surface consists of particles with a power-law size distribution (Sugita et al. 2019; Michikami et al. 2019), whereas there is a large number of particles with a size of several centimeters in the subsurface (Arakawa et al. 2020; Kadono et al. 2020b). The fact that the maximum particle size observed in the ejecta curtain caused by the SCI impact was several decimeters (Kadono et al. 2020b) suggests that not all boulders would be ejected by excavation flow in the SCI crater formation process and larger boulders should be left inside the SCI crater. Therefore, the particles inside the SCI crater are a mixture of boulders larger than several decimeters from the surface layer and a large number of smaller particles with several centimeters from the subsurface layer. Since the cumulative size distribution of particles inside the crater in Fig. 4 appears not to be a straight line, we assume that it consists of two curves: the curve on the larger side of the boundary represents the size distribution of residual boulders from the surface layer and the curve on the smaller side represents the size

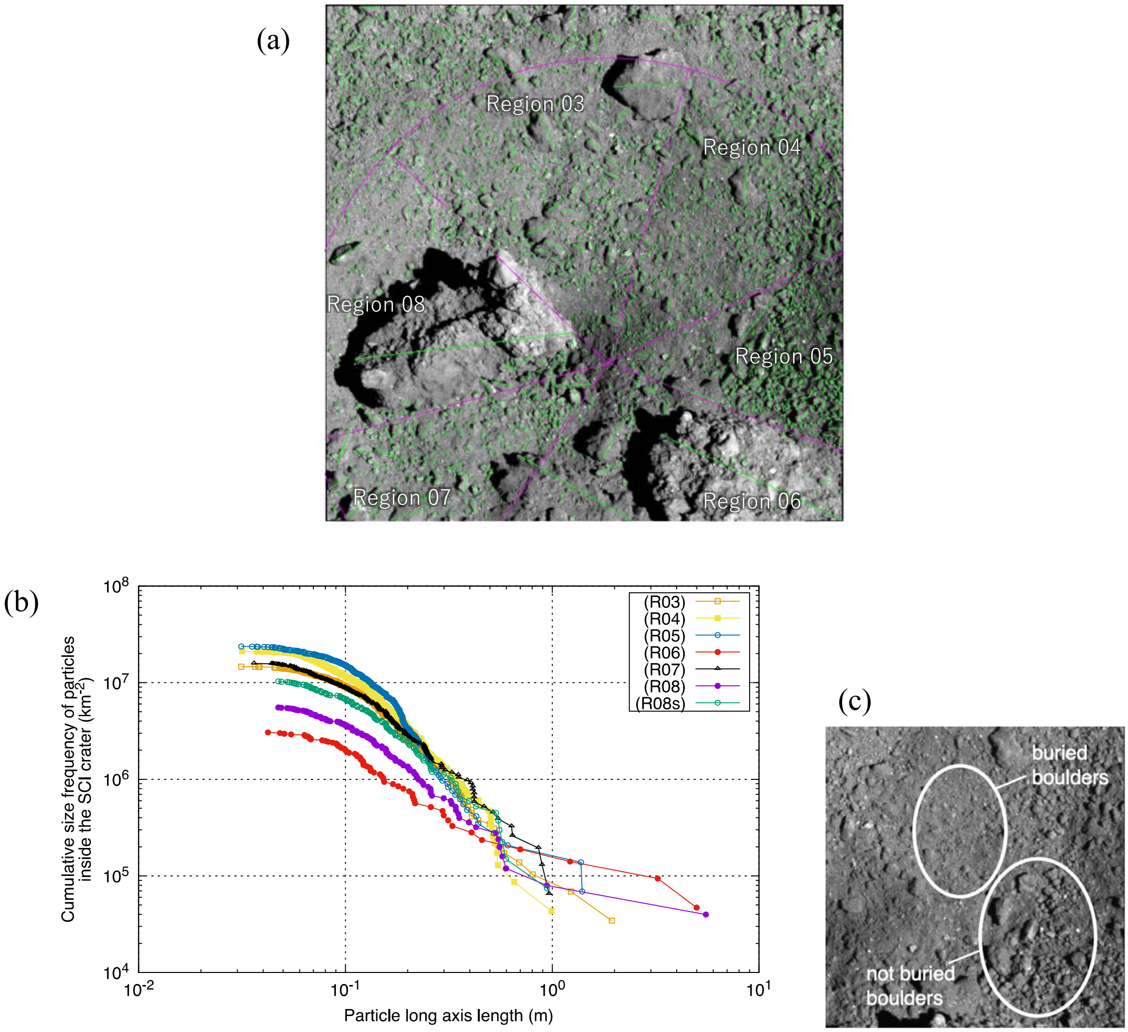

Fig. 3 **a** High-resolution image of the SCI crater interior taken by ONC-T (hyb2_onc_20190613_020224_tvf_l2c.fit). The crater outline is drawn by a purple arc, and the crater interior is divided into 6 azimuthal segments by six purple lines drawn from the center radially. Each region is named to be Region 03, 04, 05, 06, 07, and 08 clockwise. **b** Variation of cumulative size frequency distributions of particles inside the SCI crater. **c** Enlarged photo of the west side of Region 04 and Region 05

distribution of particles in the subsurface layer (the lower panel of Fig. 3b in Kadono et al. 2020b). The boundary between these curves is not definitively determined, but it should exist at a size of several decimeters. If the boundary exist at a size larger than the maximum particle size in the ejecta curtain (several decimeters), the particle size distribution inside the crater should be higher than the distribution outside the crater but in fact it is lower, while, if the boundary is smaller enough than the maximum size in the curtain, the particle size distribution inside the crater should have a flat region at sizes smaller than several decimeters, but in fact it changes with sizes smaller than several decimeters (Fig. 4). Moreover, as shown in Fig. 2b, the deposition of ejecta from the crater is remarkable at small sizes below ~ 0.5 m, suggesting that the number of the particles smaller than ~ 0.5 m is large in the subsurface layer. Therefore, we assume the boundary of 0.5 m.

The size distribution of particles smaller than 0.5 m, i.e., the size distribution in the subsurface layer, appears not to be a straight line but a curve convex on top and would have a form exhibiting a characteristic size. To evaluate the characteristic size of particles in the subsurface layer, we used an exponential form, which explicitly shows a characteristic size x_c as $\exp[-x/x_c]$. We fitted $A\exp[-x/x_c]$, where A is also a fitting parameter, to the curve on the smaller side between 0.08 and 0.5 m using the least squares method and obtained x_c of 0.085 m. This

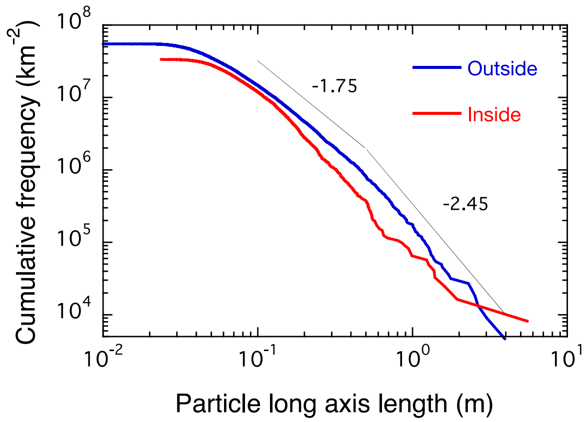

Fig. 4 Cumulative size–frequency distributions of particles inside the SCI crater (red curve) and outside the SCI crater (blue curve). The distribution of particles inside the crater is the sum of the distributions of particles in Regions 03 — 08, as shown in Fig. 3b. The distribution of particles outside the crater is the sum of the distributions of 1.0R–3.0R shown in Fig. 2a. The slopes of the distribution of particles at sizes larger than 0.5 m and between 0.1 m and 0.5 m are — 2.45 and — 1.75, respectively

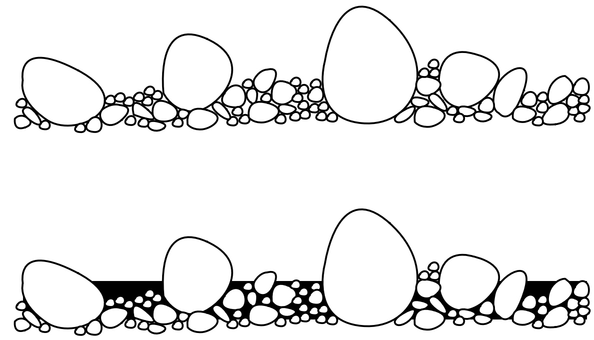

Fig. 5 Surface of Ryugu before (upper) and after (lower) ejecta deposition. When the surface is covered with ejecta, small-sized particles are obscured

is consistent with the in situ observation of the ejecta curtain (Kadono et al. 2020b; Wada et al., 2021). Thus, the size distribution of particles in the subsurface layer differs from that of the surface layer, and the subsurface layer includes a large number of small particles with a characteristic size of ~ 0.085 m, which lie around the SCI crater as ejecta blanket. It should be noted that the size distribution has not been determined at sizes smaller than ~ 5 cm from the imaging dataset. Wada et al. (2021) found that the ejecta curtain in the SCI impact contained relatively few particles smaller than ~ 1 mm. This suggests that there are relatively few particles smaller than ~ 1 mm in the subsurface layer.

Effect of ejecta deposition on the particle size distribution of the surface layer

The ejecta from the SCI crater is deposited around the crater (Arakawa et al. 2020; Honda et al. 2021). In fact, Fig. 2b shows the radial variation of particle size distribution outside the SCI crater. In this section, we investigate the influence of ejecta deposits on the slope of the size distribution and verify the claim that the size distribution is affected by finer ejecta from nearby craters that bury some small particles, as stated by Sugita et al. (2019) and Michikami et al. (2019).

We consider a situation where fine ejecta deposits and covers the particles below a horizontal plane (Fig. 5). Cutting out a 2-dimensional slice (cross-section) of a D dimensional fractal structure embedded into a 3-dimensional space usually leads to a D–1 dimensional object (e.g., Mandelbrot 1975; Vicsek 1992). Since the cumulative size frequency distribution of particles on Ryugu is a power-law form, $Ax^{-\alpha}$, where A and α are constants and x is the size of particles, the apparent size distribution of particles partially buried in the ejecta would also be a power-law with an exponent of $-(\alpha-1)$. Therefore, if the size distribution of particles is affected by finer ejecta from the SCI crater burying some particles, the difference between the slope of the apparent size distribution and the slope of the original distribution is expected to be 1.

We assume that no boulders larger than 0.5 m outside the crater were buried by the ejecta deposition and that the size distributions of boulders larger than 0.5 m were not significantly affected, so that we define the cumulative size distribution of all boulders larger than 0.5 m shown in Fig. 4 as the original size distribution before the SCI impact. This assumption is made because the maximum size of the ejecta from the crater was several decimeters (Kadono et al. 2020b), the average deposition thickness is at most ~ 0.5 m (Honda et al. 2021), and Fig. 2b shows that the effect of ejecta deposition on the size distribution can be recognized at sizes smaller than, at least, 0.5 m. Fitting a power-law form $Ax^{-\alpha}$ to the original size distribution, we obtain $1.7 \times 10^5\ x^{-2.45\pm0.01}$, where x is the boulder size in the unit of meter. It is noted that the exponent α of 2.45 is similar to the value of 2.65

Table 2 Exponents γ and $\alpha-\gamma$

Distance (R)	Exponent γ	Exponent $\alpha-\gamma$
1.0–1.5	1.862 ± 0.004	0.59 ± 0.01
1.5–2.0	1.686 ± 0.001	0.77 ± 0.01
2.0–2.5	1.736 ± 0.004	0.72 ± 0.01
2.5–3.0	1.626 ± 0.005	0.83 ± 0.01

obtained by Michikami et al. (2019) from the size distribution of boulders larger than 5 m.

The cumulative size frequency distributions after the SCI impact at sizes smaller than 0.5 m shown in Fig. 2a exhibit the apparent size distribution, $x^{-\gamma}$, where γ is a constant and is expected to be α–1. We fit a power-law form to the apparent size distributions at sizes smaller than 0.5 m using the least squares method. The obtained γ and the difference between α and γ are listed in Table 2. All values of $\alpha - \gamma$ are nearly 1, but slightly smaller. The difference from 1 can be interpreted as a result of the deposition of the ejecta not cutting out completely a 2-dimensional cross-section. This occurs probably because the ejecta is not only composed of unresolved fine particles (including particles with a few tens of centimeters) and/or the surface of the deposited ejecta layer is not uniform.

Thus, it is plausible that the ejecta deposit created by the SCI impact affects the size distribution of particles outside the crater: fine particles of the subsurface layer origin are included in the ejecta from the SCI crater, and the deposition of these fine particles buries some particles on the surface of Ryugu and changes the slope of the size distributions.

Difference in particle size distributions between the subsurface and the outermost surface

Figure 4 shows that the particle size distribution inside the SCI crater is always lower than that outside the crater at sizes smaller than 1 m. Supposing that the size distribution inside the SCI crater at small sizes is corresponding to that in the subsurface layer as in the previous section, Fig. 4 implies that the particle size distribution in the subsurface is always lower than that on the surface of Ryugu. This suggests that the first hypothesis (segregation) is the most plausible of the 3 proposed by Kadono et al. (2020b) and presented in the Introduction section. Moreover, Kitazato et al. (2021) found the small difference in composition of the materials between the surface of Ryugu and the inside of the SCI crater by the near-infrared observations. The segregation hypothesis is consistent with this observational outcome because it results in the same composition of the surface and subsurface layers. Therefore, in the following, we consider the process responsible for this two-layered structure based on the segregation hypothesis.

We consider the situation where the fast rotation model is applied to Ryugu (Watanabe et al. 2019; Hirabayashi et al. 2020; Sugiura et al. 2021). Spin-up of spherical Ryugu consisting of highly cohesive particles is assumed and landslides had been induced producing its axisymmetric top shape (Sugiura et al. 2021). The centrifugal force acting on the particles on the surface of Ryugu is $F_c\cos\phi$, where F_c is the centrifugal force at the equator and ϕ is the latitude. The force along the surface F_ϕ is $F_c\cos\phi\sin\phi$, large at mid-latitudes, moderate at low and high latitudes, and zero at the poles and equator. The particle flow along the surface driven by F_ϕ can be an along-slope flow as shown in Fig. 6. The flow velocity would be slower at high latitudes, greater at mid-latitudes, and

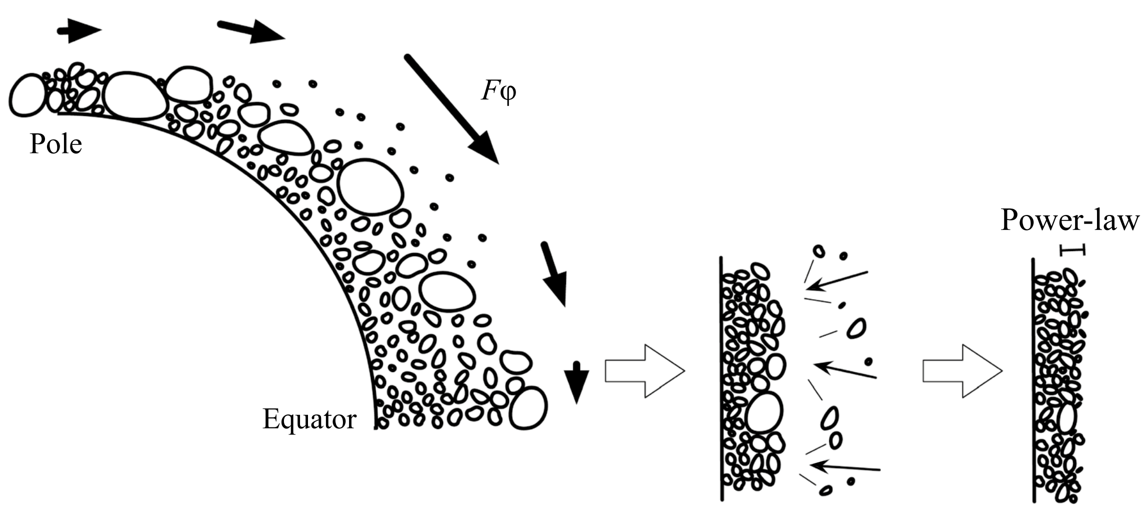

Fig. 6 Schematic illustration of Ryugu's surface formation process. The flow along the surface is driven by F_φ as an along-slope flow. As a result, segregation occurs and creates a vertically decreasing distribution of particles in size along the depth. Finer particles may acquire large random velocities to escape from the asteroid. The fragments with a power-law size distribution will then be produced by impacts. Thus, a 2-layered structure will be formed; an outermost surface layer consisting of the fragments with a power-law size distribution and a subsurface layer having a large number of particles with sizes within a specific range

slower again at low latitudes toward the equator. When a large number of particles are flowing, they collide with each other, are agitated, and then have a random velocity (e.g., Kadono et al. 2020a; Nakazawa et al. 2021). Hence, when the particles move along the surface by F_{ϕ}, they will be agitated and have a random velocity. This is similar to a situation in Brazil nut effect where vertical convection and size segregation occur (e.g., Mitani et al. 2004). The size of the particles would vertically decrease (the upper panel of Fig. 4 in Kadono et al. 2020b). The velocity of the flow would determine the maximum size of the particles in the flow. On the other hand, there may be a lower limit to the size of the particles in the flow because particles with large random velocities due to the agitation can escape the asteroid. Therefore, particles of a certain size range would accumulate in a segregated state near the equator. After slowing down of the rotation, the impact cratering disrupted the large particles on the surface and produced fragments having a power-law size distribution, and an outermost surface layer composed of these fragments was formed. Thus, the structure became an outermost surface layer consisting of particles with a power-law size distribution and a subsurface layer consisting of particles with a characteristic size. Consequently, the material on the outermost surface and in the subsurface layer is the same, but the size distribution differs.

Finally, it is important to compare the above results for Ryugu with that for another well-investigated top-shaped C-complex sub-kilometer asteroid Bennu. Although NASAs OSIRIS-REx, which observed and collected samples from Bennu, did not conduct an impact experiment, it did create – 8 m–diameter crater with the sampling operation (Lauretta et al. 2022). Their observations found a relatively high abundance of smaller particles on the surface (Lauretta et al. 2022). The fact that the 2 asteroids with different spin-state histories [i.e., recent spin down for Ryugu (Sugita et al. 2019; Morota et al. 2020) and current spin up on Bennu (Hergenrother et al. 2019; Nolan et al. 2019)] exhibit a similar fine-grain-rich subsurface layer at different latitudes [– 56° on Bennu (Lauretta et al. 2022) and – 8° on Ryugu (Arakawa et al. 2020)] is interesting. The combination of spin changes and latitudes makes these 2 artificially excavated locations erosional in terms of mass movement. Thus, some similar processes might have worked on Ryugu and Bennu. Since there are many other possibilities to account for this observed similarity in the two excavated sites; however, more analyses based on other observational data are needed for a decisive conclusion.

Summary

We examine the size distribution of particles inside and outside the SCI crater based on the images taken by the optical navigation camera onboard the Hayabusa2 spacecraft. The circumferential variation in particle size distribution inside the SCI crater is recognized. We interpret that major circumferential variation is the effect of large boulders inside the SCI crater that existed prior to the impact. The size distribution of particles inside the SCI crater also shows the subsurface layer beneath the SCI impact site had a large number of particles with a characteristic size of – 9 cm, which is consistent with the previous evaluations. On the other hand, the size distribution outside the SCI crater exhibits the radial variation, indicating that the particle size distribution is controlled by ejecta deposition around the SCI crater. The slope of the size distribution outside the crater at sizes smaller than 0.5 m differs from the slope of the size distribution on the surface of Ryugu at sizes larger than 0.5 m by approximately 1 or slightly less. This is consistent with the claim that the subsurface layer is rich in fine particles and that some particles on the surface are buried in the fine particles of the subsurface origin included in ejecta from the SCI crater. Thus, the size distributions inside and outside the crater reveal the difference in size distribution between the surface and subsurface layers: the subsurface layer is rich in small particles with – 9 cm in size while the particles on the surface have a power-law size distributions with shallower slopes at smaller sizes due to the deposition of fine ejecta from the subsurface layer. Finally, we qualitatively discuss the gravitational flow of particles on the surface of Ryugu as a process responsible for this difference in particle size distribution between the surface and the subsurface layers. The occurrence of segregation in the gravitational flow caused by fast rotation of Ryugu is plausible.

Supplementary Information

The online version contains supplementary material available at https://doi.org/10.1186/s40623-022-01713-3.

Additional file 1: Fig. S1. Overview of the slope around the SCI impact site.

Acknowledgements

The authors would like to thank all members of Hayabusa2 mission team for their support of the data acquisition. We also thank two anonymous reviews for helpful comments. The authors are grateful to M. Koga for creating the figures.

Author contributions
KO and NS conducted the ONC-T data analysis, and KO, NS, TKa, MA, RH, KW, KS, YS, KI, and YY contributed to data preparation, interpretation of results, and writing of the manuscript. KO, NS, TKa, MA, RH, KW, KS, YS, KI, YY, TS, HI, YTs, SN, YTa, MH, HY, CO, and YI developed and operated SCI. RH, YY, TM, SK, ET, YC, KY, HSa, MM, MY, TKo, HSu, CH, and SS performed the ONC-T data acquisitions and reductions. NS, TKa, MA, KS, and SS designed the paper and completed the manuscript. All authors read and approved the final manuscript.

Funding
This study was not supported.

Availability of data and materials
The datasets used and/or analyzed during the current study are available from the corresponding author on reasonable request.

Declarations

Competing interests
The authors declare that they have no competing interests.

Author details
[1]JAXA Space Exploration Center, Japan Aerospace Exploration Agency, Sagamihara, Japan. [2]Department of Planetology, Kobe University, Kobe, Japan. [3]Institute of Space and Astronautical Science, Japan Aerospace Exploration Agency, Sagamihara, Japan. [4]Department of Basic Sciences, University of Occupational and Environmental Health, Kitakyusyu, Japan. [5]Department of Information Science, Kochi University, Kochi, Japan. [6]Planetary Exploration Research Center, Chiba Institute of Technology, Narashino, Japan. [7]Aichi Toho University, Nagoya, Japan. [8]Department of Space and Astronautical Science, Graduate University for Advanced Studies (SOKENDAI), Hayama, Kanagawa, Japan. [9]Department of Earth and Planetary Science, The University of Tokyo, Tokyo, Japan. [10]Department of Physics, Rikkyo University, Tokyo, Japan. [11]Instituto de Astrofísica de Canarias, Tenerife, Spain. [12]Laboratoire d'Etudes Spatiales et d'Instrumentation en Astrophysique, Observatoire de Paris, Meudon, France. [13]National Institute of Advanced Industrial Science and Technology, Tokyo, Japan. [14]School of Science and Technology, Meiji University, Kawasaki, Japan. [15]School of Computer Science and Engineering, The University of Aizu, Aizu-Wakamatsu, Japan. [16]Department of Complexity Science and Engineering, The University of Tokyo, Tokyo, Japan.

Received: 15 March 2022 Accepted: 29 September 2022
Published online: 17 October 2022

References

Arakawa M et al (2020) An artificial impact on the asteroid (162173) Ryugu formed a crater in the gravity-dominated regime. Science 368:67–71
Harris AW, Fahnestock EG, Pravec P (2009) On the shapes and spins of "rubble pile" asteroids. Icarus 199:310–318
Hergenrother CW et al (2019) The operational environment and rotational acceleration of asteroid (101955) Bennu from OSIRIS-REx observations. Nature Comm 10:1291
Hirabayashi M, Scheeres DJ (2019) Rotationally induced failure of irregularly shaped asteroids. Icarus 317:354–364
Hirabayashi M et al (2020) Spin-driven evolution of asteroid's top-shapes at fast and slow spins seen from (101955) Bennu and (162173) Ryugu. Icarus 352:113946
Honda R et al (2021) Resurfacing processes on asteroid (162173) Ryugu caused by an artificial impact of Hayabusa2's small carry-on impactor. Icarus 366:114530
Kadono T et al (2020a) Crater-ray formation through mutual collisions of hypervelocity-impact induced ejecta particles. Icarus 339:113590
Kadono T et al (2020b) Impact experiment on asteroid (162173) Ryugu: structure beneath the impact point revealed by in situ observations of the ejecta curtain. ApJ Letters 899:L22
Kameda S et al (2017) Preflight calibration test results for optical navigation camera telescope (ONC-T) onboard the Hayabusa2 space craft. Space Sci Rev 208:17–31
Kikuchi S et al (2022) Site selection for the Hayabusa2 artificial cratering and subsurface material sampling on Ryugu. Planet Space Sci 219:105519
Kitazato K et al (2021) Thermally altered subsurface material of asteroid (162173) Ryugu. Nat Astron 5(3):246–250. https://doi.org/10.1038/s41550-020-01271-2
Lauretta D et al (2022) Spacecraft sample collection and subsurface excavation of asteroid (101955) Bennu. Science 377:285–291
Mandelbrot BB (1975) Stochastic models for the earth's relief, the shape and the fractal dimension of the coastlines, and the number-area rule for islands. Proc Nat Acad Sci USA 72:3825–3828
Michel P et al (2020) Collisional formation of top-shaped asteroids and implications for the origins of Ryugu and Bennu. Nature Comm 11:2655
Michikami T et al (2019) Boulder size and shape distributions on asteroid Ryugu. Icarus 331:179–131
Mitani NK, Mattutis HG, Kadono T (2004) Density and size segregation in deposits of pyroclastic flow. Geophys Res Lett 31:L15606
Morota T et al (2020) Sample collection from asteroid (162173) Ryugu by Hayabusa 2: implications for surface evolution. Science 368:654–659
Nakazawa K, Okuzumi S, Kurosawa K, Hasegawa S (2021) Modeling early clustering of impact-induced ejecta particles based on laboratory and numerical experiments. Planet Sci J 2:237
Nolan MC et al (2019) Detection of rotational acceleration of Bennu using HST light curve observations. Geophys Res Lett 46:1956–1962
Sugita S et al (2019) The geomorphology, color, and thermal properties of Ryugu: implications for parent-body processes. Science 364:252
Sugiura K, Kobayashi H, Watanabe S, Genda H, Hyodo R, Inutsuka S (2021) SPH simulations for shape deformation of rubble-pile asteroids through spinup: the challenge for making top-shaped asteroids Ryugu and Bennu. Icarus 365:114505
Vicsek T (1992) Fractal growth phenomena. World Scientific, Singapore
Wada K et al (2021) Size of particles ejected from an artificial impact crater on asteroid 162173 Ryugu. Astrono Astrophy 647:A43
Walsh KJ, Richardson DC, Michel P (2008) Rotational breakup as the origin of small binary asteroids. Nature 454:188–191
Watanabe S et al (2019) Hayabusa2 arrives at the carbonaceous asteroid 162173 Ryugu—a spinning top-shaped rubble pile. Science 364:268–272

Publisher's Note